Proceedings of the 8th World Congress on Mechanical, Chemical, and Material Engineering (MCM'22)
Prague, Czech Republic – July 31, 2022 - August 02, 2022
Paper No. HTFF 174
DOI: 10.11159/htff22.174

Additive Manufacturing of Capillary-Driven Two-Phase Cold Plates

Jana Catuche[1], Mohammad Reza Shaeri[1], Michael C. Ellis[2]
[1]Department of Mechanical Engineering, University of the District of Columbia, Washington, DC 20008, USA
jana.catuche@udc.edu; mohammadreza.shaeri@udc.edu
[2]Advanced Cooling Technologies, Inc., Lancaster, PA 17601, USA
mike.ellis@1-act.com

Abstract – An additively manufactured capillary-driven two-phase cold plate was fabricated for use in a hybrid two-phase cooling system (HTPCS). The pumped two-phase loop continuously supplies the cold plate with a liquid refrigerant (R245fa), which is transported by capillary action through a wick structure to the heat source. High heat flux cooling is then provided by evaporation at the menisci formed within the wick. The cold plate includes eight heaters that are located at the top and bottom surface of the cold plate. The main significance of the HTPCS lies within cold plate, or evaporator, which prevents flooding of the evaporator wick by balancing pressure drop between the liquid supply manifold and wick, while separating the liquid supply region from the vapor generation region with a non-permeable barrier (NPB). This separation allows for heat transfer by evaporation rather than boiling and enables high heat flux transport. The cold plate, integrated with wick structures and the NPB, is made of an aluminum alloy (AlSi10Mg) through one single direct metal laser sintering process. The present study is performed as a proof-of-concept to evaluate the cooling performance of the additively manufactured cold plate in a recently developed HTPCS developed by the authors. The motivation of this work is to reduce the current multiple labor-intensive fabrication processes related to previous versions of this cold plate into only one single process. The cold plate removes ~ 210 W/cm^2 from the heaters; however, the inconsistent trends of thermal resistances, as well as different thermal resistances among heaters, indicate that there are effects caused by external parameter(s) that adversely affect the wicking performance of the evaporation region. Although further detailed research is required to address discrepancies among thermal resistances, current limitations in the fabrication process, such as using internal supports inside the cold plate as well as limitations to decrease the pore size below a threshold value, are identified as possible reasons for inconsistency in thermal resistances. Such limitations need to be addressed through further research into the additive manufacturing processes.

***Keywords*:** Hybrid two-phase cooling; Pumped two-phase loop; Capillary-driven two-phase cooling; Additive manufacturing; Cold plate.

1. Introduction

The rapid miniaturization of electronic components, along with an increase in their power, have resulted in challenges with the thermal management of electronic devices. Commonly used active and passive two-phase cooling technologies may not be sufficient for cooling ever-shrinking electronic devices with heat dissipation exceeding 1000 W/cm^2 [1-3]. Capillary-driven two-phase systems like heat pipes and vapor chambers achieve high heat transfer coefficients without the need of an external power; however, they are prone to severe challenges related to their capillary limit [4]. Although pumped two-phase technologies like micro/minichannel heat sinks have been demonstrated to remove large heat fluxes while operating with low pumping power, they are prone to flow boiling instabilities that have catastrophic impacts on the thermal performance of the cooling system [5]. As a result, to respond to the challenges of thermal management for high heat flux electronic components, hybrid two-phase cooling systems (HTPCSs) have been proposed [6].

Recently, Shaeri et al. [7] developed a HTPCS that integrated the benefits of pumped two-phase cooling and capillary-driven two-phase cooling, as schematically shown in Fig. 1. The pumped two-phase loop consisted of a copper cold plate, a reservoir, two heat exchangers, and a pump. The components of the loop were connected to each other through stainless steel tubes and the working fluid was the refrigerant R245fa. At various locations of the loop, temperatures and pressures were measured using T-type thermocouples and pressure transducers, respectively. The loop was equipped with a control valve, a filter, and a flowmeter as well. Inside the cold plate, the cooling mechanism was capillary-driven evaporation from the heat transfer regions that were sintered copper powder wick structures. The cold plate included multiple heaters, and each individual heater was cooled by its own evaporation region located underneath the heaters. However, the major significance of the developed HTPCS in [7] was preventing flooding of the evaporator wicks by using a non-permeable barrier (NPB) made of a rubber that inhibited flow of the liquid over the wicks. Fig. 2 illustrates the schematic of the cold plate along with evaporator wicks on one side of the cold plate and the NPB. The pumped two-phase loop continuously supplied liquid to the cold plate. A portion of the liquid that was transported through the wicks from outside the NPB was used for evaporation inside the NPB. The remaining liquid was excess flow that could be two-phase flow due to boiling within the liquid supply manifold but outside the NPB. As illustrated in Fig. 2, the excess flow could turn inside the cold plate from the gap between the NPB and the wall of the ring (i.e., the structure of the cold plate used to hold the evaporators). Throughout the cooling process, the vapor inside the NPB and the excess flow outside of the NPB were separated from each other and exited the cold plate through the respective manifolds, as shown in Fig. 1. The vapor generated from the interior section of the NPB was pushed to the condenser by the vapor pressure inside the NPB. Because of a lower vapor quality in the excess flow compared with the flow in the vapor line, the excess flow was returned directly to the reservoir. To avoid cavitation in the pump, a condenser was used between the reservoir and pump to ensure that the inlet flow to the pump was a single-phase liquid. Then, the liquid refrigerant was pumped into the cold plate and the loop was completed. Shaeri et al. [7] characterized the performance of their proposed HTPCS using eight high heat flux heaters, four at the top and four at the bottom surface of the cold plate. The HTPCS removed heat fluxes over 970 W/cm^2 over areas less than 0.12 cm^2, and the thermal resistance was as low as 0.09 K-cm^2/W for all heaters. Also, the cooling system operated with a low pumping power below 1.0 W, which is a significant advantage of a pumped two-phase cooling.

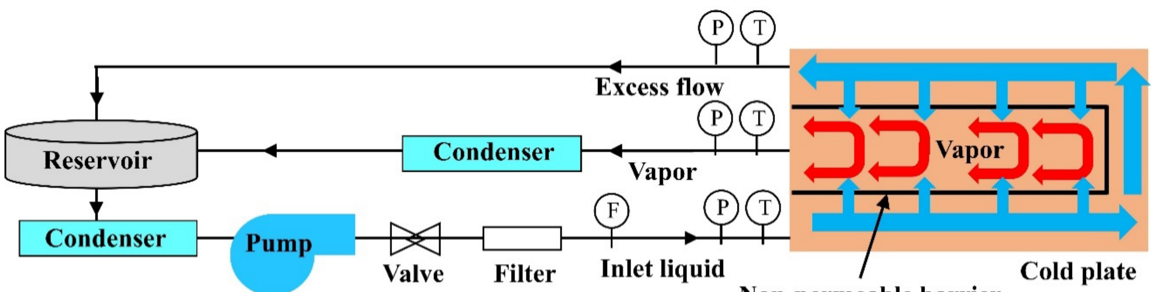

Fig. 1: Schematic of the developed HTPCS in [7]. T, P, and F indicate T-type thermocouples, pressure transducers, and flowmeter, respectively. Reprinted from [7] with permission from Elsevier.

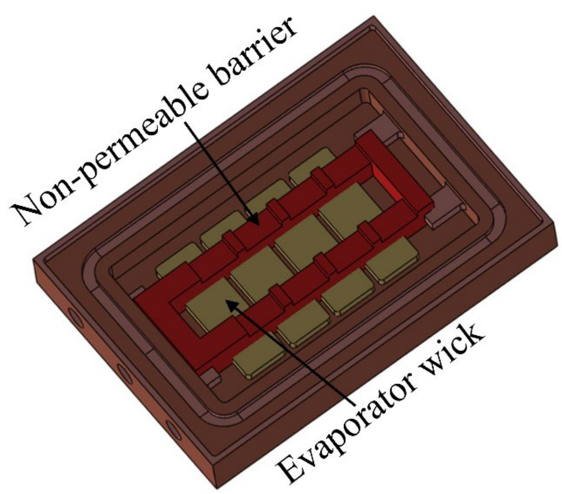

Fig. 2: Inside the cold plate of HTPCS in [7] without the top substrate. Reprinted from [7] with permission from Elsevier.

Despite high thermal performances of the HTPCS in [7], the manufacturing complexity of the cold plate is a big challenge for commercialization of this cooling technology. The cold plate was developed through multiple labor-intensive intensive steps, mainly as: (1) computer numerical control (CNC) machining to fabricate a ring structure including features features to support the NPB, (2) CNC machining to make substrates where evaporator wicks are fabricated, (3) CNC machining to fabricate mandrel(s) for preparing evaporator wicks, (4) high-temperature sintering process for fabricating evaporator wicks, (5) a precise cutting process (e.g., water jet) to make very thin and precise cuts on the NPB, (6) inserting inserting the NPB inside the ring and keep it stationary in place, and (7) a metal bonding process for joining substrates to the to the ring. Each of these processes is costly, time-consuming, and requires a separate facility. In addition, the performance of the cold plate strongly depends on the accuracy of the individual processes. For example, any gap between the rubber (NPB) and the surface of the evaporator may result in liquid entering the interior part of the NPB and flooding the wicks. Such destructive effect can happen by a movement of rubber during bonding of the substrates and the ring. Furthermore, inconsistency in the characteristics of the wick structures is highly possible due to current traditional sintering processes that result in random characteristics for wick structures.

To overcome the above challenges, an additively manufactured cold plate integrated with evaporator wicks and NPB is fabricated in the present study. The additive manufacturing technique reduces multiple labor-intensive fabrication processes of the cold plate into only one single process, which substantially reduces the complexity, time, and cost of fabrication process, and is an essential step for commercialization of HTPCS.

2. Proposed Cold Plate

Figs. 3 and 4 illustrate the additively manufactured cold plate that is fabricated in the present study. As one of the advantages of the presented cold plate, the gap between the surface of the cold plate and wicks is completely filled with a metal NPB, which is structurally robust. The cold plate is made of an aluminum alloy (AlSi10Mg) through direct metal laser sintering (DMLS) process. AlSi10Mg is an additive manufacturable alloy with a reasonably high thermal conductivity [8]. The cold plate includes eight heaters with four of them located at the top surface of the cold plate and the remaining at the bottom surface. The order of heaters on the top surface is specified in Fig. 3(a). The same order exists on the bottom surface as such that heater 5 is located under heater 1. The refrigerant R245fa is used as the working fluid. The operation of the HTPCS is the same as that of the cooling system in [7]. The pedestals in Fig. 3 are the locations where heaters are placed. Heaters C200N50Z4 (Anaren Inc.) are mechanically pressed into the pedestals, and the space between the surface of each pedestal and heater is filled with a thermal grease. The pedestals have a converging structure to reduce the footprint area of the heat source to that of the commercially available transistor GS66502B (GaN Systems Inc.). The reason for using a converging pedestal is unavailability of off-the-shelf high-power heaters with the same footprint size of transistor. The transistor footprint area is used for the data reduction.

The thermal performance of the HTPCS is characterized by the thermal resistance of each heater (R_i), as follows:

$$R_i = \frac{T_{s,i} - \left(\frac{T_{in} + T_r}{2}\right)}{q_i} \tag{1}$$

where $T_{s,i}$, T_{in}, and T_r represent the temperature of the ith heater, temperature of liquid at the inlet of cold plate, and the reservoir temperature, respectively. Also, q_i is the heat flux to the ith heater, which is calculated as follows:

$$q_i = \varphi \frac{Q_{E,i}}{A} \tag{2}$$

where $Q_{E,i}$ is the electrical heat input to the ith heater, and A is the footprint area of the transistor. In the present study, $A = 0.12\ \mathrm{cm}^2$ and is the same for all heaters. Also, φ represents the ratio of the effective heat absorbed by the working fluid to the total electrical heat input to the cold plate $\left(Q_{E,t}\right)$, as follows [9]:

$$\varphi = \frac{\rho \dot{V} c_p (T_{out} - T_{in})}{Q_{E,t}} \tag{3}$$

where ρ, $\dot{V}$, c_p, and T_{out} are the liquid density, volume flow rate, specific heat, and outlet temperature, respectively. To calculate φ, a series of single-phase heat transfer experiments were conducted prior to the two-phase heat transfer tests; then, the mean value of 0.8 was used for φ from a range of heat transfer ratios that were obtained.

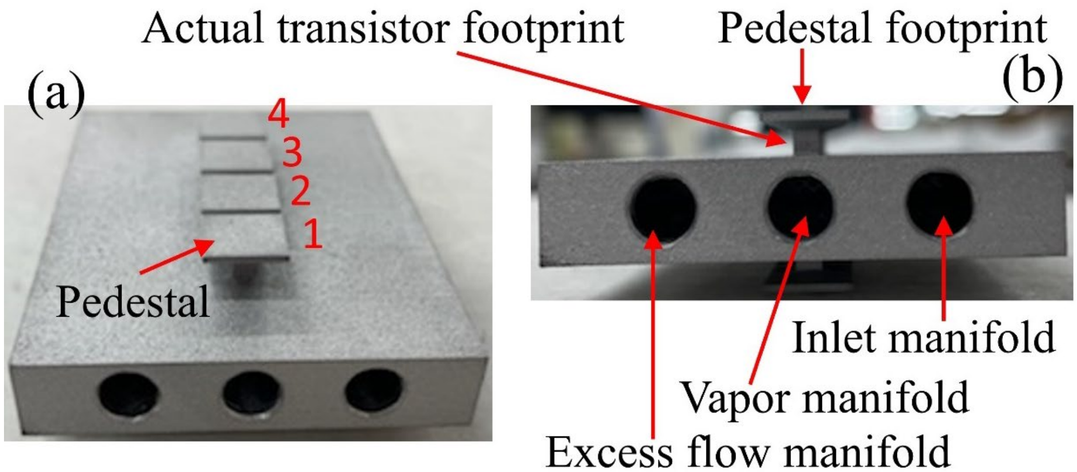

Fig. 3: Additively manufactured cold plate. Numbers in (a) indicate the order of heaters on one side of the cold plate. Underneath of heaters 1 to 4 are heaters 5 to 8.

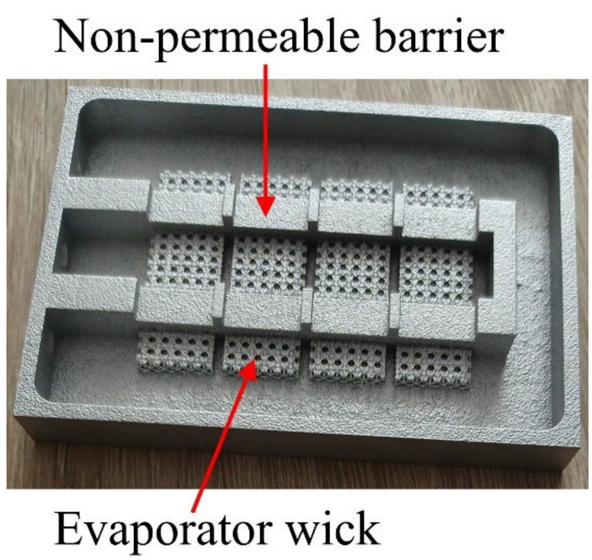

Fig. 4: Inside the additively manufactured cold plate without the top substrate

3. Results

The entire two-phase loop was checked for any possible leaks prior to charging the loop with the refrigerant. The experiment was conducted at a flow rate of ~ 1.0 L/min. The inlet temperature was maintained within the range of 35 −

37.7 °C. The electrical heat input to each heater was increased by regulating the voltage of the variable transformer. The data was collected at each heat input when a steady state condition was reached. The steady state corresponds to negligible changes in the temperatures measured by thermocouples during a 15-minute period of operation. Signals from the thermocouples, pressure transducers, flowmeter, and heaters were collected by a LabVIEW Data Acquisition system. When the liquid was pumped into the cold plate, a portion of the liquid that was outside the NPB (shown in Fig. 4) was transported into the interior part of the NPB through the evaporator wicks. The excess flow was turned inside the cold plate from the gap between the NPB and the cold plate wall and exited the cold plate from separate outlet.

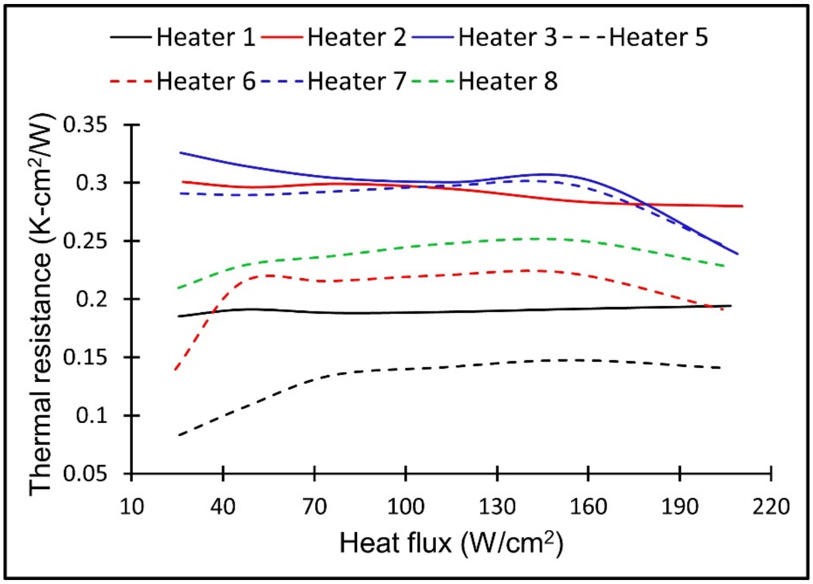

Fig. 5: Thermal resistances at different heat fluxes. The results for heater 4 are omitted because it was not operating properly during the tests.

Fig. 5 illustrates the thermal resistances as a function of heat fluxes. During the experiments, heater 4 was not properly operating; as a result, corresponding data to heater 4 is not shown. The present HTPCS removes heat fluxes up to 210 W/cm^2, which is a high heat flux value. While corresponding thermal resistances of heaters 1 and 5, which are the closest heaters to the inlet, are reasonably low, other thermal resistances are slightly higher. Since the cold plate and wick structures in [7] were fabricated with copper, a lower thermal resistance is expected from the cold plate due to higher thermal conductivity of copper compared with the aluminum alloy. However, the main difference between the present results with those in [7] is the trend of thermal resistances at different heat fluxes. While the thermal resistances were almost the same for all the heaters in [7] and monotonically decreased by increasing the heat flux, inconsistent trends among thermal resistances of the different heaters are observed in the present cold plate. Although detailed research is required to address the reason of inconsistent thermal resistances among the heaters, limitations of the current fabrication process can be one of the main reasons. Since the goal of this project is to fabricate the cold plate through one single additive manufacturing process without relying on conventional fabrication processes, the manufacturing faced some challenges mainly because some parts of the cold plate were not accessible. Due to manufacturing complexity, some internal supports were implemented inside the cold plate to allow for additive manufacturing, which were not part of the original design. While at this moment, it is difficult to interpret the impacts of these internal structures on the overall performance of the cold plate, it is possible that these structures affect liquid transport inside the wicks by partial blocking of some wicks. Another major limitation of the present manufacturing process is a lack of enough control on wick structure and pore size, which does not allow fabrication of wicks with a desired pore size. However, characteristics of a sintered wick structure can be highly controlled by properly packing the copper particles in the mandrels for fabrication of wicks. As a result, the current limitations of additive manufacturing are identified as the main reasons for low thermal performance of the present cold plate. Through further progression in additive manufacturing, effective and compact cold plates can be fabricated to address the shortcoming of the present cold plate.

4. Conclusion

To reduce multiple labor-intensive fabrication processes of a capillary-driven two-phase cold plate into one single process, an additively manufactured cold plate integrated with wick structures and a NPB was fabricated through DMLS process. The cold plate was used in a HTPCS to remove heat from multiple heaters. Although a high heat flux of ~ 210 W/cm^2 was removed from the heaters, inconsistent thermal resistances among the heaters indicate that the removal of heat was impacted by some elements most likely from limitations in the additive manufacturing process. Implementing internal supports inside the cold plate may cause partial blockage of some wicks, which adversely affects the wicking ability of the evaporators. Another limitation is a lack of control on developing wick structures with desired properties resulting from additive manufacturing. Further detailed research is required to resolve fabrication challenges of capillary-driven cold plates.

Acknowledgements

The financial support from NASA MUREP Small Business Technology Transfer (M-STTR) (Grant# 80NSSC21K1883), the National Science Foundation-CREST Award (Contract #HRD-1914751), and the Department of Energy/National Nuclear Security Agency (DE-FOA-0003945) are gratefully acknowledged. Also, the authors are thankful to Mr. Maksym Demydovych and Mr. Philip Martin for their support in the experiments.

References

[1] M. R. Shaeri, D. Attinger, R. W. Bonner III, "Vapor chambers with hydrophobic and biphilic evaporators in moderate to high heat flux applications," *Appl. Therm. Eng.*, vol. 130, pp. 83-92, 2018.

[2] K. Luo, W. Li, J. Ma, W. Chang, G. Huang, C. Li, "Silicon microchannels flow boiling enhanced via microporous decorated sidewalls," *Int. J. Heat Mass Transfer*, vol. 191, p. 122817, 2022.

[3] M. R. Shaeri, D. Attinger, R. Bonner, "Feasibility study of a vapor chamber with a hydrophobic evaporator substrate in high heat flux applications," *Int. Commun. Heat Mass Transfer*, vol. 86, pp. 199-205, 2017.

[4] K. Baraya, J. A. Weibel, S. V. Garimella, "Heat pipe dryout and temperature hysteresis in response to transient heat pulses exceeding the capillary limit," *Int. J. Heat Mass Transfer*, vol. 148, p. 119135, 2020.

[5] J. Tang, Y. Liu, B. Huang, D. Xu, "Enhanced heat transfer coefficient of flow boiling in microchannels through expansion areas," *Int. J. Therm. Sci.*, vol. 177, p. 107573, 2022.

[6] C. Park, A. Vallury, J. Perez, "Advanced hybrid cooling loop technology for high performance thermal management," *In 4th International Energy Conversion Engineering Conference and Exhibit (IECEC)*, p. 4059. 2006.

[7] M. R. Shaeri, R. W. Bonner, M. C. Ellis, "Thin hybrid capillary two-phase cooling system," *Int. Commun. Heat Mass Transfer*, vol. 112, p. 104490, 2020.

[8] R. R. J. Selo, S. Catchpole-Smith, I. Maskery, I. Ashcroft, C. Tuck, "On the thermal conductivity of AlSi10Mg and lattice structures made by laser powder bed fusion," *Addit. Manuf.*, vol. 34, p. 101214, 2020.

[9] D. Deng, R. Chen, Y. Tang, L. Lu, T. Zeng, W. Wan, "A comparative study of flow boiling performance in reentrant copper microchannels and reentrant porous microchannels with multi-scale rough surface," *Int. J. Multiphase Flow*, vol. 72, pp. 275-287, 2015.